Japanese Journal of Applied Physics
Vol. 46, No. 9A, 2007, pp. 5951–5953

Brief Communication

A Fringe-Field Driven Hybrid Aligned Nematic Liquid Crystal Display for Narrow Viewing Angle Display

Je Woo RYU, Young Jin LIM, Youn Hak JEONG, Kyungmi KIM[1], Gi-Dong LEE[1]*, and Seung Hee LEE[†]

BK-21 Polymer BIN Fusion Research Team, Research Center for Advanced Materials Development, School of Advanced Materials Engineering, Chonbuk National University, Chonju, Chonbuk 561-756, Korea
[1]*Department of Electronics Engineering, Dong-A University, Pusan 607-735, Korea*

(Received March 29, 2007; accepted June 2, 2007; published online September 7, 2007)

Liquid crystal displays (LCDs) that exhibit a high image quality at the normal direction only were investigated. For this purpose, a hybrid aligned nematic liquid crystal (LC) cell driven by a fringe electric field was chosen, and its electro-optic characteristics with an optimal cell structure were evaluated. The device showed a high light efficiency of 90%, a low driving voltage and a narrow viewing angle $< 30°$ in terms of a CR of 2 : 1 along the horizontal direction, which is suitable for private display applications. [DOI: 10.1143/JJAP.46.5951]

KEYWORDS: liquid crystal display, fringe-field switching, narrow viewing angle

Liquid crystal displays (LCDs) are widely used as interfaces between humans and machines. Recently, considerable effort using new LC modes such as in-plain switching (IPS),[1] fringe-field switching (FFS),[2–5] and multi-domain vertical alignment modes has been made to improve the image quality of the LCDs.[6,7] On the other hand, there have been many studies of LCDs in which image quality can be controlled from a wide to narrow viewing angle[8–10] or narrow viewing LC mode only.[11]

For application displays for the purpose of privacy protection on an individual hold, a narrow viewing angle is essential particularly in horizontal direction. In addition, for portable displays, a low driving voltage (V_{op}) in which the V_{op} is defined as a voltage that gives rise to the maximal transmittance and high transmittance are also required.

Many LC modes have been studied in order to realize a very narrow viewing angle. Among them, a hybrid aligned nematic (HAN) LCD driven by fringe-field (named HAN-FFS mode)[12–14] was investigated. In HAN-FFS mode, the pixel electrodes with some width (w) exist with a distance (l) between them above a common electrode with a passivation layer between them only on the bottom substrate. In this device, the transmittance is proportional to $\sin^2(2\psi)\sin^2(\delta/2)$, where ψ is the angle between the LC optic axis and the axes of the crossed polarizers. δ is the phase difference between the ordinary and extraordinary rays, and is equal to $\pi d\Delta n/\lambda$, where d and Δn are the thickness and birefringence of the LC layer, respectively, and λ is the wavelength of the incident light. In the off state, hybrid aligned nematic LCs exist under crossed polarizers. However, the optic axis of the cell is coincident with the polarizer axis. Therefore, the cell appears black at the normal direction, as shown in Fig. 1. In the on state, the fringe-field, which has both a horizontal and vertical component, is generated between the pixel and common electrodes. The dielectric torque between the LC and the field drives the LC to rotate. The optic axis of the LC then deviates from the polarizer axis, giving rise to transmittance.

The device exhibits a low V_{op} because the LC on the top substrate is aligned vertically, i.e., the LCs near the top substrate can rotate in any direction due to nonexistence of azimuthal anchoring. Furthermore, a LC with positive dielectric anisotropy (+LC) is essential for this device to achieve a low V_{op} and fast response time. However, when a +LC is used, the transmittance has a lower transmittance than that of the twisted nematic (TN) mode and the HAN-FFS mode using an LC with negative dielectric anisotropy.

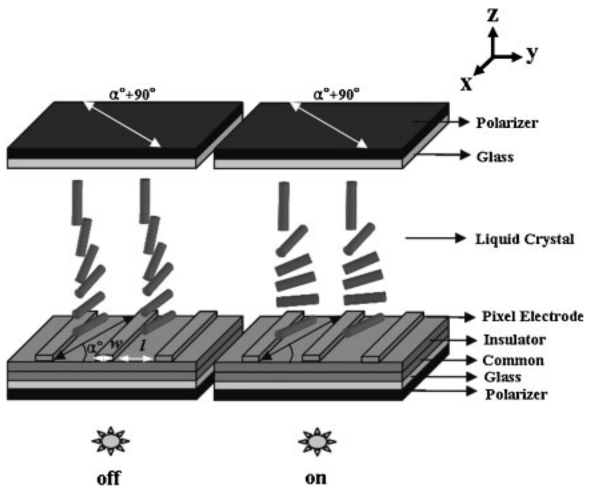

Fig. 1. Schematic of the cell structure of the HAN-FFS cell in the off and on states using a LC with positive dielectric anisotropy.

This study examined the electrode structure and optimal cell conditions exhibiting a high transmittance even with +LC, and investigated their electro-optic characteristics. This work proposes LCD exhibiting a distorted displayed image quality in the oblique directions but a high image quality at the normal direction with good electro-optic characteristics.

There are two approaches for realizing a narrow viewing angle LCD. The first is to suppress light transmittance in the white and gray states so that the display becomes dark in the oblique viewing direction. The second is to generate strong light leakage at dark state such that there is excessive brightness greater than that at the normal direction in the oblique viewing direction, causing a deterioration of the image quality by a gray scale inversion. The latter approach was chosen in this device.

As shown in Fig. 1, the device has electrodes only on the bottom substrate such that the pixel electrodes exist in a slit form above the counter electrode in planar form with a passivation layer between them. Therefore, the field strength

*E-mail address: gdlee@dau.ac.kr
†E-mail address: lsh1@chonbuk.ac.kr

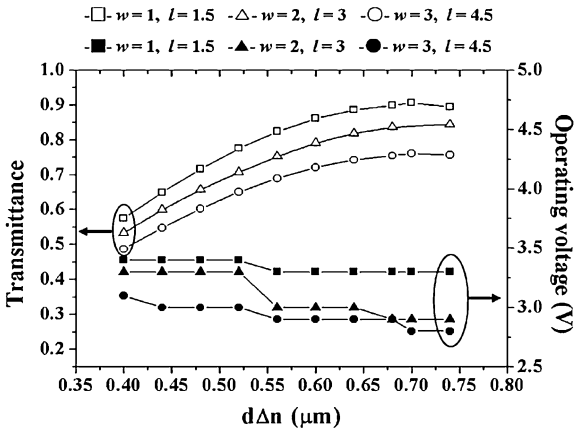

Fig. 2. Calculated result of the normalized maximal transmittance and operation voltage as a function of $d\Delta n$.

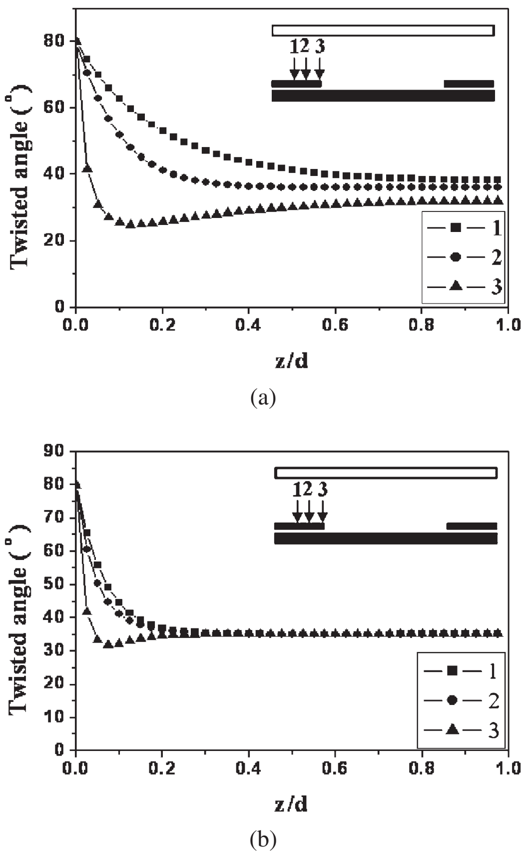

Fig. 3. Profile of the LC molecules in a twist angle according to the electrode structure: (a) $w = 3\,\mu$m, $l = 4.5\,\mu$m and (b) $w = 1\,\mu$m, $l = 1.5\,\mu$m.

and shape strongly depend on the pixel electrode width as well as the distance between them. This means that the dielectric torque to rotate the LC depends on the electrode position and structure.

Figure 2 shows how the calculated V_{op} and normalized maximal transmittance change according to the electrode structure and cell retardation value ($d\Delta n$). Here, the thickness of the passivation layer was 0.290 μm. A 2×2 extended Jones matrix at a wavelength of 550 nm was used for the optical calculation. Here, the LC (dielectric anisotropy $\Delta\varepsilon = 8.2$, elastic constants $K_1 = 9.7$ pN, $K_2 = 5.2$ pN, $K_3 = 13.3$ pN) and a cell gap of 4 μm were used. Furthermore, the birefringence of the LC was changed to calculate the transmittance. For this calculation, the rubbing angle (α) was assumed to be 80° with respect to the horizontal component of a fringe-electric field. The transmittance of the single and parallel polarizer was 41 and 35%, respectively.

As indicated in Fig. 2, the normalized maximal transmittance was strongly dependent on the electrode structure and cell retardation value. When the w and l between the electrodes was 3 and 4.5 μm, respectively, and the retardation of the LC cell is 0.70 μm, the cell showed a transmittance of 0.76 with an operating voltage of 2.8 V. When w and l were decreased to 2 and 3 μm, respectively, the cell showed a transmittance of 0.84 with a V_{op} of 2.9 V when the retardation of the LC cell is 0.74 μm. As the w and l is further decreased to 1 μm and 1.5 μm, respectively, the transmittance is almost the same along electrode positions due to a strong horizontal electric field, giving rise to a high transmittance of 0.90. However, the V_{op} increased to 3.3 V when the retardation of the LC cell was 0.70 μm. The transmittance is as high as that of the TN mode but the V_{op} is comparable to that of the TN mode and less than those of the other LC modes. This suggests that this device is suitable for portable displays. In particular, the electrode width becomes narrower while keeping the ratio l/w, and the cell retardation value that gives the maximal transmittance increases but the V_{op} increases.[15)]

In order to determine how a decrease in the pixel electrode and distance between electrodes increases the transmittance, the profile of the LC molecules was calculated, i.e., the twist angle according to the electrode structure with a cell retardation value that allows maximum transmittance, as shown in Fig. 3. When $w = 3\,\mu$m, the maximum twisted angle from the initial position was strongly dependent on the electrode position such that it was approximately 55° (= 80° − 25°) near the bottom substrate at the edge of the electrode (position 3). When w is 1 μm, the maximum twisted angle > 40° from the initial twist angle of 80° occurs near the bottom electrode surface below $z/d = 0.2$ irrespective of the electrode positions (here $z/d = 0$ and 1 indicates the bottom and top surfaces of the LC layers, respectively). For both LC cells, the retardation of the LC cell was 0.70 μm.

Figure 4 shows the iso-luminance curves in the white and dark states, as well as the iso-contrast curves depending on the electrode structure with an optimal cell retardation value of 0.70 μm. The luminance curves were indicated as 70, 50, and 30% of the maximum luminance in the dark and white state, respectively. The luminance at the white state for both cells with $w = 3\,\mu$m, $l = 4.5\,\mu$m, and $w = 1\,\mu$m, $l = 1.5$ μm decreased rapidly in the cross-sectional plane of the azimuthal directions from 45 to 225° compared with those in the cross-sectional plane of the azimuthal directions from 135 to 315° as the viewing direction changes from the normal to oblique viewing direction. The strong light leakage in the dark state occurs at both the right and left directions with respect to the rubbing direction. There is little difference in the iso-luminance curves of the white and dark states between the cells with $w = 3$ and 1 μm.

Considering the iso-contrast curves, both cells exhibit a CR of 2 : 1 at a polar angle of approximately 30° in the horizontal direction (along y-direction in Fig. 1), and a CR > 10 : 1 at a polar angle < 20° in the horizontal direction. Both cells show very narrow viewing angle characteristics compared with the conventional LC cells

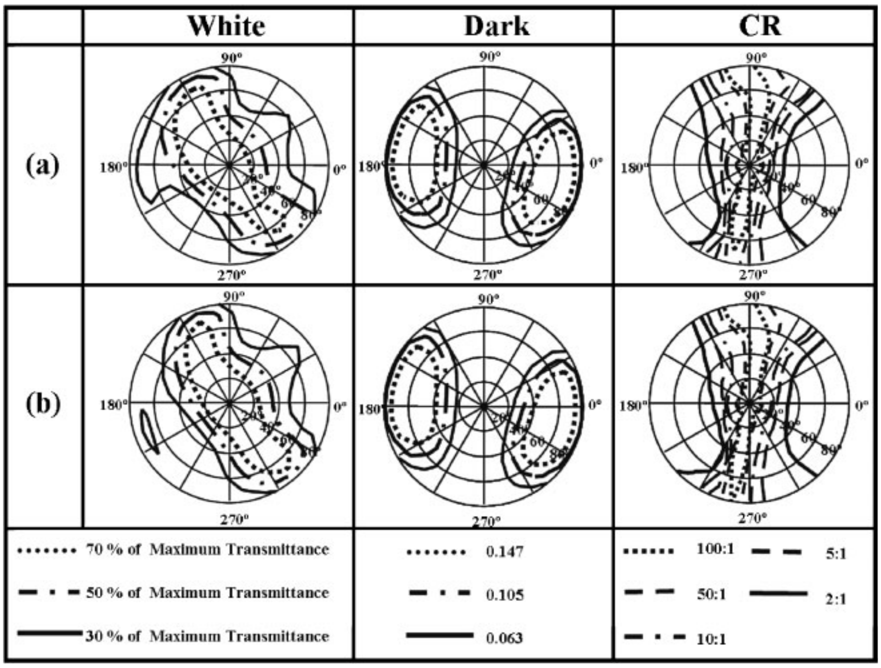

Fig. 4. Iso-luminance curves in the white and dark states, as well as the iso-contrast curves at an incident wavelength of 550 nm: (a) $w = 3\,\mu m$, $l = 4.5\,\mu m$ and (b) $w = 1\,\mu m$, $l = 1.5\,\mu m$.

such as the TN and FFS modes. These narrow viewing angle characteristics arise from the decreased luminance in the white state and the strong light leakage in the dark state.

Finally, the degree of gray scale inversion was examined by calculating the viewing angle dependence of the eight gray levels in the horizontal direction in which the transmittance was divided into eight different levels for the cell with $w = 3\,\mu m$ and $l = 4.5\,\mu m$, and a retardation value $0.70\,\mu m$. As shown in Fig. 5, a gray-scale inversion > 10 and $-15°$ begins to occur. Furthermore, excessive brightness and darkness compared with the transmittance at the normal direction also exist along the left and right horizontal direction, respectively. This suggests that the displayed image will be strongly distorted in the horizontal direction when the oblique viewing angle exceeds more than 20° from the normal axis.

In summary, a display for the purpose of privacy protection on an individual hold are essential and LC mode was developed for this purpose, which exhibits a high transmittance, low driving voltage and a narrow viewing angle $< 20°$ along the horizontal direction.

This work is supported financially by the Ministry of Education and Human Resources Development (MOE), the Ministry of Commerce, Industry and Energy (MOCIE) and the Ministry of Labor (MOLAB) through the fostering project of the Lab of Excellency.

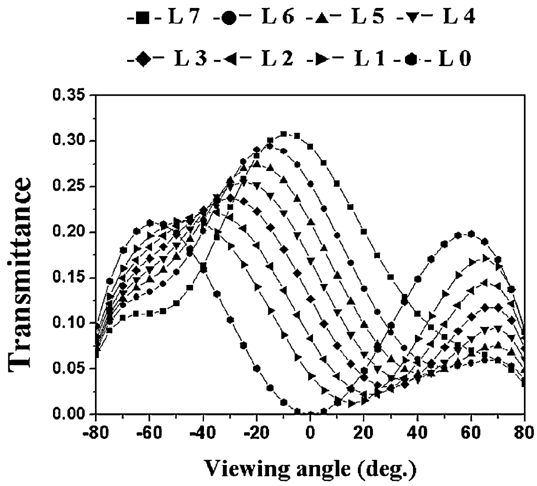

Fig. 5. Viewing angle dependence of the 8 gray levels along the horizontal direction for a cell with $w = 3\,\mu m$ and $l = 4.5\,\mu m$.

1) M. Oh-e and K. Kondo: Appl. Phys. Lett. **67** (1995) 3895.
2) S. H. Lee, S. L. Lee, and H. Y. Kim: Proc. 18th Int. Display Research Conf., 1998, p. 371.
3) S. H. Lee, S. L. Lee, and H. Y. Kim: Appl. Phys. Lett. **73** (1998) 2881.
4) S. H. Lee, S. L. Lee, H. Y. Kim, and T. Y. Eom: SID Int. Symp. Dig. Tech. Pap. **30** (1999) 202.
5) S. H. Lee, S. M. Lee, H. Y. Kim, J. M. Kim, S. H. Hong, Y. H. Jeong, C. H. Park, Y. J. Choi, J. Y. Lee, J. W. Koh, and H. S. Park: SID Int. Symp. Dig. Tech. Pap. **32** (2001) 484.
6) A. Takeda, S. Kataoka, T. Sasaki, H. Chida, H. Tsuda, K. Ohmuro, T. Sasabayashi, Y. Koike, and K. Okamoto: SID Int. Symp. Dig. Tech. Pap. **29** (1998) 1077.
7) Y. Tanaka, Y. Taniguchi, T. Sasaki, A. Takeda, Y. Koibe, and K. Okamoto: SID Int. Symp. Dig. Tech. Pap. **30** (1999) 206.
8) Y. Hisatake, Y. Kawata, and A. Murayama: SID Int. Symp. Dig. Tech. Pap. **36** (2005) 1218.
9) H. S. Jin, H. S. Chang, J. K. Park, S. K. Yu, D. S. Lee, and I. J. Chung: SID Int. Symp. Dig. Tech. Pap. **37** (2006) 729.
10) E. Jeong, Y. J. Lim, J. M. Rhee, G.-D. Lee, K. H. Park, H. C. Choi, and S. H. Lee: Appl. Phys. Lett. **90** (2007) 051116.
11) Y. Sun, Z. Zhang, and H. Ma: Jpn. J. Appl. Phys. **41** (2002) 3878.
12) S. H. Hong, Y. H. Jeong, H. Y. Kim, and S. H. Lee: Jpn. J. Appl. Phys. **40** (2001) L272.
13) S. H. Hong, H. Y. Kim, J. H. Kim, S. H. Nam, M. H. Lee, and S. H. Lee: Jpn. J. Appl. Phys. **41** (2002) 4571.
14) W. C. Kim, Y. H. Jeong, and S. H. Lee: Jpn. J. Appl. Phys. **43** (2004) 637.
15) I. H. Yu, I. S. Song, J. Y. Lee, and S. H. Lee: J. Phys. D **39** (2006) 2367.